APPENDIX 6.

Optically stimulated luminescence (OSL) dating of fluvial sediments from the Medway Valley.

J.-L. Schwenninger, F. Wenban-Smith, M.R. Bates and R.M. Briant

Summary: A total of 27 samples collected from Pleistocene aggregate deposits in north Kent and southeast Essex were used for dating by optically stimulated luminescence (OSL). The samples originated from fluvial terrace deposits associated with the river Medway in the Medway Valley north of Maidstone, the Hoo peninsula and the southeast quarter of Essex, up to Clacton-on-Sea.

The OSL age estimates were obtained on sand-sized quartz grains and palaeodose determinations were made using a single-aliquot regenerative dose (SAR) measurement protocol. For each sample the environmental dose rate was calculated from the concentrations of radioactive elements derived by ICP-MS analysis using a fusion sample preparation method. The concentrations of uranium, thorium and potassium were well above detection limits and the samples and their luminescence characteristics were generally considered to be well suited for OSL dating.

Keywords: Fluvial sediments – Geochronology – Medway Valley – OSL dating – Pleistocene – Quaternary.

Contents

1 Introduction

The River Medway has been in existence for over 2 M years, draining northward from the centre of the Weald. For most of this period the landscape of southern England has been substantially different to the present day, and the course of the Medway has varied considerably. Until circa 500 ka, the Thames Estuary did not exist, and the Medway flowed north across the Hoo peninsula to enter the North Sea near Ipswich. Following this, Britain was affected by a major ice age and a thick ice sheet covered East Anglia, advancing south towards London. This had the effect of diverting the Thames, which at that point was flowing east across Essex and Suffolk, further south. The new course of the Thames joined with the Medway in the vicinity of the Hoo peninsula, and then the joined Thames/Medway flowed across southeast Essex to enter the North Sea at Clacton. Since then, the joined channel has migrated progressively further southward, leaving a series of palaeo-Thames/Medway deposits preserved between Southend and the Dengie Peninsula.

Through time and due to a combination of erosional down-cutting and uplift of the earth's crust in southeast England, the Medway has flowed at progressively lower levels. Sand and gravel deposits laid down by earlier courses of the Medway are now preserved as "terraces" high above the banks of the present river channel. In some places, such as the Hoo peninsula, a "staircase" of terrace deposits is preserved, with successively older deposits occurring higher up the valley sides. The river would often have been similar to rivers found in Arctic Canada at the present day, with numerous shallow (braided) channels crossing a gravel plain. These terrace deposits contain fossil animal bones and flint artefacts, caught up when they were formed, and thus provide evidence about the climate and the environment in this ancient time. In many places these Middle and Late Pleistocene fluvial sand/gravel aggregate deposits have also produced Palaeolithic archaeological evidence.

The OSL dating programme forms an important part in the development of a regional Palaeolithic research framework and aims to provide an integrated chronology for the stratigraphic sequence characterizing the sand and gravel aggregate deposits in the palaeo-Medway River region. Fieldwork was undertaken in key areas identified from the mapped terrace deposits. This involved digging test pits with a JCB and collecting suitable samples for palaeo-environmental studies and optically stimulated luminescence (OSL) dating. Sample processing and luminescence measurements were made at the Luminescence Dating Laboratory in the Research Laboratory for Archaeology and the History of Art at the University of Oxford. In-situ radioactivity measurements were made by project personnel using a gamma-ray spectrometer acquired by English Heritage. Separate moisture content samples were collected in order to make suitable correction for the attenuation effect of water. These measurements were carried out by B. Briant at the Department of Geography, Queen Mary, University of London.

A series of 27 samples were submitted for OSL dating and further details regarding individual samples are presented in table 1.1. Replicate samples were collected on most occasions but only one pair of duplicate samples was considered for dating.

Laboratory code	Field code	Site name	Replicate samples	In situ NaI γ-ray spectrometry
X2447	BLNG05-01	Barling Gravel Pit	Yes	Yes
X2449	BLNG05-03	Barling Gravel Pit	Yes	Yes
X2451	BLNG05-05	Barling Gravel Pit	Yes	Yes
X2455	BURN05-01	Burnham Wick Farm	Yes	Yes
X2457	BURN05-03	Burnham Wick Farm	Yes	Yes
X2459	CG05-01	Cudmore Grove	Yes	Yes
X2460	CG05-02	Cudmore Grove	Yes	Yes
X2461	CG05-03	Cudmore Grove	No	Yes
X2463	CG05-05	Cudmore Grove	Yes	Yes
X2466	DOGF05-02	Doggets Farm	Yes	Yes
X2467	DOGF05-03	Doggets Farm	Yes	Yes
X2478	MLF05-01	Medway Lafarge	No	Yes
X2553	CLBG05-01	Clubb's Pit, Grain	Yes	Yes
X2555	CLBG05-03	Clubb's Pit, Grain	Yes	Yes
X2557	CLBG05-05	Clubb's Pit, Grain	Yes	Yes
X2559	CXTN405-01	Cuxton	Yes	Yes
X2561	CXTN405-03	Cuxton	Yes	Yes
X2563	CXTN405-05	Cuxton	Yes	Yes
X2566	KMP05-02	Kingsmead Park	Yes	Yes
X2580	NHFM05-01	Newhall Farm	Yes	Yes
X2582	RHLLF05-01	Ringshill Farm	Yes	Yes
X2588	WTHF05-02	Whitehouse Farm	Yes	Yes
X2589	DGFM05-03	Dagnam Farm	Yes	No
X2591	MCKY05-01	Mackays Court Farm	No	No
X2672	NHL05-01	New Hythe	Yes	Yes
X2674	RHLLF05-05	Ringshill Farm	Yes	Yes
X2677	SLM05-02	Sandling Place	No	No

Table 1.1 OSL sample details. Replicate samples were collected in most instances but only one pair of duplicates from Cudmore Grove was submitted for dating (X2459 and X2460).

2 Methods

2.1 The physical basis of luminescence dating

When ionising radiation (predominantly alpha, beta or gamma radiation) interacts with an insulating crystal lattice (such as quartz or feldspar), a net redistribution of electronic charge takes place. Electrons are stripped from the outer shells of atoms and though most return immediately, a proportion escape and become trapped at meta-stable sites within the lattice. This charge redistribution continues for the duration of the radiation exposure and the amount of trapped charge is therefore related to both,

the duration and the intensity of radiation exposure. Even though trapped at meta-stable sites, electrons become 'free' if the crystal is subjected to heat or exposed to light. Once liberated, a free electron may become trapped once again or may return to a vacant position caused by the absence of a previously displaced electron (a 'hole'). This latter occurrence is termed 'recombination' and the location of the hole is described as the 'recombination centre'. As recombination occurs, a proportion of the energy of the electron is dissipated. Depending upon the nature of the centre where recombination occurs, this energy is expelled as heat and/or light. Therefore, when the crystal grain is either heated or illuminated following natural or artificial laboratory irradiation (the 'dose') the total amount of light emitted (luminescence) is directly related to the number of liberated electrons and available recombination sites. This is the fundamental principle upon which luminescence dating is based.

In cases where the duration of dosing is not known (as is the case for dating), estimates can be made from laboratory measurements. The response (the sensitivity) of the sample to radiation dose (i.e. the amount of light observed for a given amount of laboratory radiation, usually β-radiation) must be established. From this relationship the equivalent radiation exposure required to produce the same amount of light as that observed following the natural environmental dose can be determined, and is termed the palaeodose or 'equivalent dose' (D_e). The palaeodose (measured in Gy) is therefore an estimate of the total dose absorbed during the irradiation period. When the dose rate (the amount of radiation per unit time, measured in μGy/a) is measured (or calculated from measured concentrations of radionuclides), the duration of the dosing period can be calculated using the equation:

$$\text{Duration of dosing period} = \text{Palaeodose} \div \text{dose rate.}$$

The technique of optical dating was first applied to quartz by Huntley *et al*. (1985), and methodological details were further developed by Smith *et al.* (1986) and Rhodes (1988). The technique was demonstrated to work well for aeolian samples by Smith et al. (1990), and has further proved to provide useful age estimates for a range of sedimentary contexts ranging from aeolian (e.g. Stokes *et al.* 1997, Aitken 1998) to glacial contexts (Owen *et al.* 1997). Further developmental research has introduced palaeosoe measurement protocols that use a 'single aliquot regenerative-dose' (SAR) protocol (Murray and Wintle 2000). These protocols generally have the potential to provide increased precision in the luminescence measurements, and may in some cases provide an indication of incomplete zeroing of the luminescence signal at the time of deposition. Recent research within the laboratory (Rhodes et al. 2003) has demonstrated the high precision and accuracy that may be achieved with this technique.

2.2 Sample preparation

The laboratory procedures were designed to yield pure quartz, of a particular grain size range, from the natural sediment samples. In order to obtain this material, samples were taken through a standard preparation procedure, as outlined below.

All laboratory treatments were performed under low intensity laboratory safe-lighting, from purpose-built filtered sodium lamps (emitting at 588 nm).

The sample was wet-sieved to a resolution of ~5μm, and the modal grain size was retained for further processing. Typically the grain sizes used for dating were 125-180 μm or 180-250μm (see Appendix 1 for details of specific samples). The chosen fraction was treated with hydrochloric acid (HCl) to remove carbonate and then treated in concentrated HF (48%) for 90 minutes. This treatment serves two purposes: (i) to dissolve feldspar grains, and (ii) to remove (etch) the outer surface of quartz grains (the only part of each quartz grain exposed during burial to natural alpha radiation). Any heavy minerals present were subsequently removed by gravity separation using a sodium polytungstate solution at 2.68 $g.cm^{-3}$. Finally, each sample was re-sieved to remove heavily etched grains. The prepared quartz was mounted on 1cm diameter aluminium discs for luminescence measurements using viscous silicone oil and small sized aliquots (2-4 mm) were prepared for each sample.

Various tests for sample purity are made. Sub-samples of the prepared material are examined using optical microscopy and the sample is exposed (within the Risø measurement system) to infrared (IR) light. Quartz generally does not produce measurable IR luminescence at room temperature whereas feldspar, which can suffer from anomalous fading of the IRSL and OSL signals, or may be less rapidly bleached in some environments, produces an intense luminescence when stimulated with IR. The presence of a strong infra-red stimulated luminescence (IRSL) signal is therefore used as an indication for the presence of feldspar contaminants and is a criterion for rejection. In the rare cases where samples are rejected due to presence of high levels of IRSL, the prepared sediment sample is treated for ~ 2 weeks in concentrated H_2SiF_6 (silica-saturated HF) which effectively dissolves non-quartz material. If following this treatment, IRSL persists then the sample is subjected to a further two week H_2SiF_6 acid treatment before proceeding to the dating phase (luminescence measurement) and the results are interpreted with caution and the possible contamination of the sample will be discussed.

The measurement sequence adopted for dating includes a post-IR blue OSL procedure (Banerjee et al. 2001) designed to deplete any feldspar contribution to the OSL signal, by preceding each OSL measurement with an IRSL measurement. The IR exposure reduces the size of feldspar contributions, besides providing an alternative means for determining the palaeodose. For samples with strong IRSL signals, significant feldspar contribution to the OSL may remain, and this is considered in the interpretation of the dates. Several samples were found to possess high IRSL intensities but following treatment with fluorosilicic acid as described above, the feldspar signal contribution was reduced to negligible levels.

2.3 The single aliquot regenerative-dose (SAR) protocol

The SAR method is a regeneration procedure where the light level of the natural signal is converted into Gy via an interpolation between regenerated (i.e. known dose) points. The natural and regenerated signals are measured using the same aliquot. Sensitivity change commonly observed in quartz TL/OSL has previously

precluded meaningful results being obtained this way. A key development reported by Murray and Wintle (2000) is that sample (aliquot) sensitivity is monitored following each OSL measurement (L_i) using the OSL response to a common test dose (S_i). Plots of $OSL1_i/OSL2_i$ provide the necessary (sensitivity change corrected) data for interpolation. The procedure is further outlined below, in Figure 2.1.

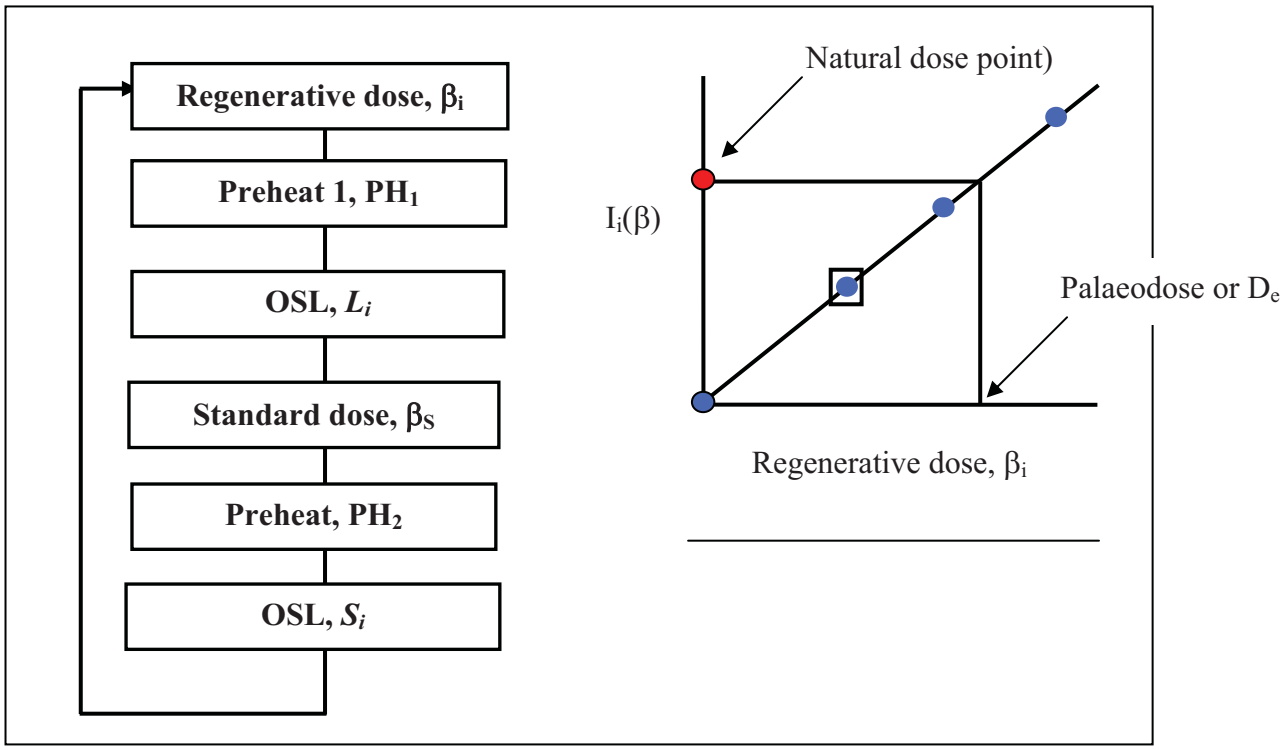

Figure 2.1 Outline of the SAR measurement protocol. The procedure illustrated here is described in further detail in the text.

Steps 1-6 are repeated n times in order to produce the data points required for interpolation (the first dose β_1 being zero, to give a measure of the natural signal). Typically n=7 (i.e. the natural plus 6 regeneration points, including one zero dose point and one repeat point). PH_1 and PH_2 are usually different although Murray and Wintle (2000) report no dependence of D_e on either (over the range of 200-280°C). The OSL signal is integrated over the initial part of the decay (to ~10% of initial intensity) and the background is taken as the light level measured at the end of each OSL measurement.

Murray and Wintle (2000) have introduced two further steps in to the measurement procedure. The first is the re-measurement of the first regenerated data point (indicated by the box in the explanatory Figure 2.1 above). The ratio of the two points (the "recycling ratio") provides an assessment of the efficacy of the sensitivity correction and the accuracy of the technique (large differences being suggestive of an ineffective technique). The recycling ratio (ideally unity) is

typically in the range 0.95-1.05. The second additional step is a measurement of the regenerated OSL due to zero dose. This value gives a measure of the degree of thermal transfer to the trap(s) responsible for OSL during pre-heating. The ratio of this value to the natural OSL value (both corrected for sensitivity change) gives the "thermal transfer ratio" and ideally this should be in the range of 0.005-0.020.

2.4 Measurement procedures and conditions

Luminescence measurements were made using automated Risø luminescence measurement equipment. There are currently three different systems within the Luminescence Dating Laboratory that can be used for routine dating, the major difference between them being the optical stimulation sources. In two systems, optical excitation is provided by filtered blue diodes (emitting ~410-510nm), and in the third a filtered Halogen lamp (emitting ~420-560nm) is used. In all three systems, infrared stimulation is also provided using either an array of IR diodes or a single IR laser diode (depending on the measurement system). Luminescence is detected in the UV region on all systems, using EMI 9635Q bialkali photomultiplier tubes, filtered with Hoya U340 glass filters. Sample irradiation is provided in all cases by sealed ^{90}Sr sources at a rate of 1.5-3 Gy/minute depending on the system used.

The mean palaeodose for each sample was obtained from 6-12 aliquots (see Appendix 3 for further details regarding the statistics used in palaeodose and error calculations). All OSL measurements were made at 125°C (to ensure no re-trapping of charge to the 110°C TL trap during measurement) for between 50 and 100s, depending on the measurement system used. The signal detected in the initial 1st to 2^{d} seconds (with the stable background count rate from the last 12 to 24 seconds subtracted) was corrected for sensitivity using the OSL signal regenerated by a subsequent beta dose (β_s). To ensure removal of unstable OSL components, removal of dose quenching effects and to stimulate re-trapping and ensure meaningful comparison between naturally and laboratory irradiated signal, pre-heating was performed prior to each OSL measurement. Following each regenerative dose (β_i) and the natural dose, a pre-heat (PH_1) at 260°C for 10s was used for all the samples. Following each test dose (β_s), a pre-heat (PH_2) of 220°C for 10s was applied (see Section 2.3 for further details of the SAR method). All the OSL measurements incorporated a post-IR blue OSL stage in which each OSL measurement is preceded by an IRSL measurement at 50°C, to reduce the effects of any residual feldspar grains (Banerjee et al., 2001) but the SAR procedure is otherwise unchanged.

For every sample, a routine preliminary series of measurements were performed on three separate aliquots prior to the main SAR measurement in order to determine their approximate palaeodose value, their internal variability, the OSL and TL signal form and sensitivity as well as the magnitude of any IRSL signals. This considerably assists in the optimal selection of regenerative and test dose values, number of aliquots to measure and the preheat combination selected. Quartz samples showing high levels of IRSL at this stage are given a further extended (usually 2 weeks) treatment in fluorosilicic acid (H_2SiF_6).

3 Results

The OSL dating results including age estimates, palaeodose and environmental dose rate measurements are summarized in Table 3.1. Further details regarding individual samples may be found in Appendix 1. Factors affecting the dose rate determinations and the statistics used in error calculations are described in more detail in Appendices 2 and 3.

OSL age estimates presented here are based on sand-sized quartz grains extracted from each sample and the measurements are derived from series of 6 or 12 aliquots per sample. Dose rates used for the age calculations were based on the results of geochemical analysis by ICP-MS using a fusion preparation method. Complementary, in-situ gamma-ray spectroscopy measurements were made at most locations (except for Sandling Place, Mackays Court Farm and Dagnam Farm) using a portable NaI γ-spectrometer acquired by English Heritage in 2005 with the aim to facilitate the collection of samples without having to call out specialist personnel from the dating laboratory on each occasion. This approach was justified in view of the anticipated nature of the fieldwork which would require numerous sampling trips in order to accommodate access to private land at relatively short notice. Initial setting-up of the instrument was performed at the Research Laboratory for Archaeology but the acquisition and analysis of individual spectra was left to project personnel.

The analysis of the spectrometry data was subsequently passed on to the dating laboratory. It is at this stage that we noticed that the spectra were characterized by a very wide background window. The typical peaks used for calibration purposes and for deriving elemental concentrations are generally well resolved but unfortunately, these are located in a very narrow total count window. Our in-house software is currently not able to cope with the spectra acquired by this particular instrument and will require changes to the code in order to accommodate the specific instrument settings and the rather unusual characteristics of the field spectra. The wide background may be due to the inadvertent resetting of the instruments gain during software installation or re-installation onto a different laptop. Although we have tried to modify the software, and spent more than two weeks doing so, we have so far failed to derive reliable concentrations which are consistent with the calibration spectra and are in broad agreement with the laboratory based elemental analyses. We are relatively confident that this problem can be overcome in the future but in the meantime, the dose rate estimates for all the samples can only be based on the results of the elemental geochemical analysis carried out on sub-samples.

Fortunately, the OSL samples were collected by field personnel with previous OSL sampling experience and where possible, samples were not taken close to sedimentary boundaries or bedrock, thus minimizing any substantial contribution from unaccounted external gamma-ray sources. The samples which are most likely to be affected by a potential problem of this nature are those located within close distance (20 cm or less) to overlying or underlying sedimentary units containing sediment of a different texture or mineralogical make-up. From the vertical position of samples and the corresponding description of the relevant sediments, the OSL age estimates most likely to be affected by this problem are: X2449, X2451,

X2587, X2565, X2465, X2467, X2455 and X245. For the above mentioned the results should at present be interpreted with caution and regarded as preliminary dates.

All the samples displayed well defined luminescence signals (see figure 3.1) and other OSL characteristics were also found to be generally well suited for SAR age determination. Very low IRSL values were observed for all the samples [mean overall IRSL/OSL ratio = 0.003; see table 3.2 for details], suggesting good quartz separation had been achieved during sample preparation. Most samples are further characterized by a predominance of the OSL fast component (see figure 3.1) as well as excellent sensitivity to laboratory induced irradiation. Positive characteristics of the luminescence properties of the Medway sediments are also evident in the low thermal transfer values (mean = 1.87 %; see table 3.2) and excellent recycling ratios (mean = 1.01) having mean ratios close to unity (see figure 3.2 and table 3.2. for details) Low inter-aliquot variability between repeat measurements of multiple aliquots prepared from the same sample was observed in most instances (see figure 3.3). Further confidence in the palaeodose estimates is given by the good agreement in estimates achieved for the paired replicate samples X2459 and X2460 (see table 3.1).

The OSL age estimates reveal one clear outlier for sample X2559 which provided a late Holocene date [1880 ± 300; AD126]. This result is in stark contrast to the remaining samples in the series which are all in line with the expected Pleistocene age. There is no indication that this sample may have been subjected to partial bleaching or may have undergone exposure to light during sample preparation. The intrusion of younger grains through bioturbation or indeed complete reworking as a result of disturbance is unlikely based on the OSL measurements alone. It seems more plausible that the sample was inadvertently collected from a genuinely younger near surface depositional context [sample depth was only 50cm] and it may in fact be associated with known Roman activity in the vicinity.

Several samples [Cudmore Grove, Doggets Farm, New Hythe and Ringshill Farm] display elevated errors compared to the other samples in the series. These are mainly associated with increased inter-aliquot variability in the palaeodose estimates. Samples from these sites would benefit from future single grain analysis in order to rule out signal interference from older grains of geological age or grains which may have retained a residual signal relating to a previous depositional context. Although high sensitivity is usually regarded as an advantage, this may also represent a problem in situations where one or a handful of ‘rogue’ contaminant grains may dominate the luminescence signal. Samples X2672 and X2674 [New Hythe and Ringshill Farm] in particular appear to be affected by this problem. For both these samples the calculated age estimates are therefore based on the low palaeodose values and are therefore more likely to represent minimum age estimates.

A further cautionary note concerns the high variability in the moisture content observed among the sediments in the Medway sample series. These were shown to vary from 3 to 18 percent. In order to account for seasonal effects and to obtain a representative average water content over the entire burial period of the sample, inflated errors were attached to the contemporary values. For samples with a

moisture content below 10 percent, the dose rate calculations are based on a systematic ± 3 percent error range so that for example in the case of a measured water content of 5 %, the actual range used to calculate the OSL date is based on a water content of 2 to 8 percent. For samples exceeding 10 percent this error range was extended to ± 5 %. In most instances, we determined the moisture content of the samples from small samples collected specifically for this purpose. These were double bagged and sealed to minimize moisture loss. Additionally we determined the moisture content from the end parts of the OSL sampling containers which were closed with rubber caps. This provided an additional check in case the sealed sample bags leaked or got punctured during transport or storage. There was generally good agreement between both sets of independent measurements although as expected, the values derived from the OSL tubes were generally slightly below those obtained for the sealed bags. For five samples [X2589, X2591, X2672, X2674 and X2677] no special water content samples were available. This includes the three samples collected from blocks or cores [X2589, X2591 and X2677] for which the water concentrations are entirely dependent upon the samples themselves and the assumption that these were well wrapped up and did not experience a substantial loss of water during storage. The values are consistent with those recorded from other samples in the series and thus there is no reason to question the modern water contents. The same may not be true of samples X2672 and X2674 which provided very low water concentrations of 1.1 and 0.6 % respectively. This may be related to the relatively shallow burial depth of both these samples [1.20 m and 0.65 m]. Such low values raise immediate suspicion although, free drainage and good permeability may well explain these results. Without having visited the site it is difficult to comment further on this issue. Generally, the net effect of underestimating the true average water content of a samples would lead to an underestimate of its true age. If some of the sites have been affected by substantial changes in hydrology, perhaps as a result of drainage in recent times, then this could have a corresponding effect on the calculated OSL dates. It would be good to clarify aspects relating to the hydrology of individual sites before publishing the final luminescence dates in a refereed journal.

Finally, it is worth highlighting the very low concentration of potassium [0.09 %] determined for sample X2672. This sample provided the oldest OSL age estimate [300.2 ka] but the date is strongly dependent on the low K content. Concentrations of U and Th are also lower but much more in line with those detected within the other samples. Preferential leaching of potassium may be invoked and it would be worthwhile further testing the sediment for disequilibrium by carrying out high resolution germanium gamma-ray spectrometry measurements on sealed or resin impregnated samples. A repeat elemental analysis by ICP-MS on a duplicate sample would also be justified in order to rule out any potential instrument problems affecting the initial set of geochemical analysis.

Field code	Laboratory code	Palaeodose (Gy)	Dose rate (mGy/a)	OSL age estimate (ka)
BLNG05-01	X2447	143.06±3.72	0.97±0.05	147.07±9.40
BLNG05-03	X2449	197.61±18.50	1.48±0.11	133.66±15.85
BLNG05-05	X2451	127.16±4.76	1.05±0.07	121.52±9.29
BURN05-01	X2455	220.31±21.71	1.77±0.13	124.79±15.46
BURN05-03	X2457	126.56±10.55	0.77±0.04	164.61±16.76
CG05-01	X2459	148.67±4.21	0.61±0.03	242.82±15.10
CG05-02	X2460	132.50±18.82	0.54±0.03	245.64±37.80
CG05-03	X2461	176.59±14.47	0.85±0.04	208.36±20.73
CG05-05	X2463	145.39±11.77	0.72±0.04	202.96±19.64
DOGF05-02	X2466	106.92±15.28	0.42±0.03	253.66±41.82
DOGF05-03	X2467	221.68±13.62	0.84±0.04	265.00±22.15
MLF05-01	X2478	240.39±13.06	1.32±0.06	181.55±13.68
CLBG05-01	X2553	188.40±8.45	0.96±0.05	196.10±14.14
CLBG05-03	X2555	205.26±12.27	1.43±0.10	143.33±13.20
CLBG05-05	X2557	191.48±11.80	1.30±0.09	147.52±13.78
CXTN405-01	X2559	2.11±0.31	1.12±0.06	1.88±0.30
CXTN405-03	X2561	200.90±6.15	0.86±0.04	232.64±13.75
CXTN405-05	X2563	169.38±11.28	0.86±0.04	197.54±17.09
KMP05-02	X2566	71.05±0.91	0.92±0.05	77.23±4.47
NHFM05-01	X2580	81.22±3.00	1.12±0.07	72.63±5.68
RHLLF05-01	X2582	227.07±9.36	1.65±0.08	137.34±9.17
WTHF05-02	X2588	296.60±7.54	1.93±0.13	153.82±11.60
DGFM05-03	X2589	292.55±17.83	1.59±0.08	183.92±14.94
MCKY05-01	X2591	268.93±11.32	1.89±0.12	142.59±11.46
NHL05-01	X2672	171.79±13.90	0.57±0.03	300.16±29.23
RHLLF05-05	X2674	242.03±22.61	0.90±0.05	268.64±29.64
SLM05-02	X2677	295.91±15.64	1.43±0.07	206.45±15.30

Table 3.1 Summary of OSL dating results. The results are based on luminescence measurements of sand-sized quartz (125-180 or 180-255μm). All samples were measured using a SAR post-IR blue OSL protocol (Murray and Wintle 2000, Banerjee et al. 2001). Dose rate calculations are based on the concentration of radioactive elements (potassium, thorium and uranium) derived from geochemical analysis by ICP-MS using a fusion sample preparation technique. The final OSL age estimates include an additional 2 % systematic error to account for uncertainties related to source calibration. Dose rate calculations are based on Aitken (1985). These incorporated beta attenuation factors (Mejdahl 1979), dose rate conversion factors (Adamiec and Aitken 1998) and an absorption coefficient for the water content (Zimmerman 1971). The contribution of cosmic radiation to the total dose rate was calculated as a function of latitude, altitude, burial depth and average over-burden density based on data by Prescott and Hutton (1994). Further details regarding individual samples may be found in Appendix 1.

Field code	Laboratory code	Mean recycling ratio	Mean Thermal transfer (%)	Percent of rejected aliquots	Mean IRSL/OSL ratio
BLNG05-01	X2447	1.05	2.25	16.7	0.003
BLNG05-03	X2449	1.00	1.95	16.7	0.004
BLNG05-05	X2451	1.01	2.39	16.7	0.005
BURN05-01	X2455	0.97	1.54	16.7	0.003
BURN05-03	X2457	1.04	1.44	16.7	0.003
CG05-01	X2459	-	-	0	0.001
CG05-02	X2460	1.01	1.01	0	0.007
CG05-03	X2461	1.02	1.16	33.3	0.002
CG05-05	X2463	0.99	0.83	50.0	0.001
DOGF05-02	X2466	1.03	1.79	33.3	0.001
DOGF05-03	X2467	0.98	1.99	16.7	0.000
MLF05-01	X2478	0.99	2.09	16.7	0.002
CLBG05-01	X2553	0.98	2.65	0	0.007
CLBG05-03	X2555	1.02	1.54	16.7	0.004
CLBG05-05	X2557	1.02	1.74	0	0.004
CXTN405-01	X2559	1.02	7.56	16.7	0.006
CXTN405-03	X2561	1.00	2.20	16.7	0.008
CXTN405-05	X2563	1.02	1.68	0	0.002
KMP05-02	X2566	1.03	1.78	0	0.005
NHFM05-01	X2580	1.04	1.80	16.7	0.004
RHLLF05-01	X2582	1.00	1.71	16.7	0.004
WTHF05-02	X2588	1.01	1.38	16.7	0.002
DGFM05-03	X2589	1.00	1.73	16.7	0.007
MCKY05-01	X2591	1.04	1.62	0	0.006
NHL05-01	X2672	0.98	1.72	16.7	0.004
RHLLF05-05	X2674	1.01	0.88	50.0	0.001
SLM05-02	X2677	0.99	0.66	33.3	0.001
		1.01	**1.87**	**16.7**	**0.003**

Table 3.2 Summary of luminescence characteristics including tests for recycling, recuperation and feldspar contamination as well as the percentage of aliquots that were rejected from the analysis.

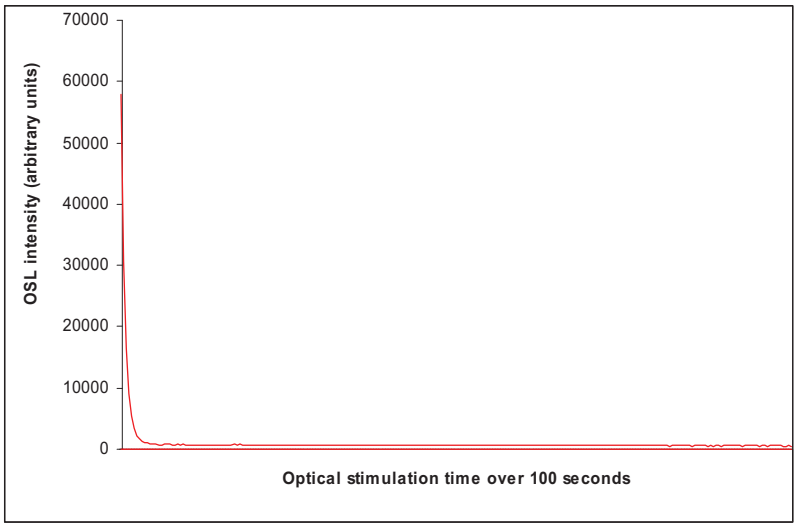

Figure 3.1 Example of a shine down curve obtained for the natural OSL signal from sample X2566 [aliquot 6] and which is typical of most of the samples analysed in this study. The signal was measured over a 100 second period and is dominated by contributions from the fast component of the OSL signal. The high signal intensity is a direct reflection of the prolonged burial period of the sample and the high OSL sensitivity of the quartz within the study area.

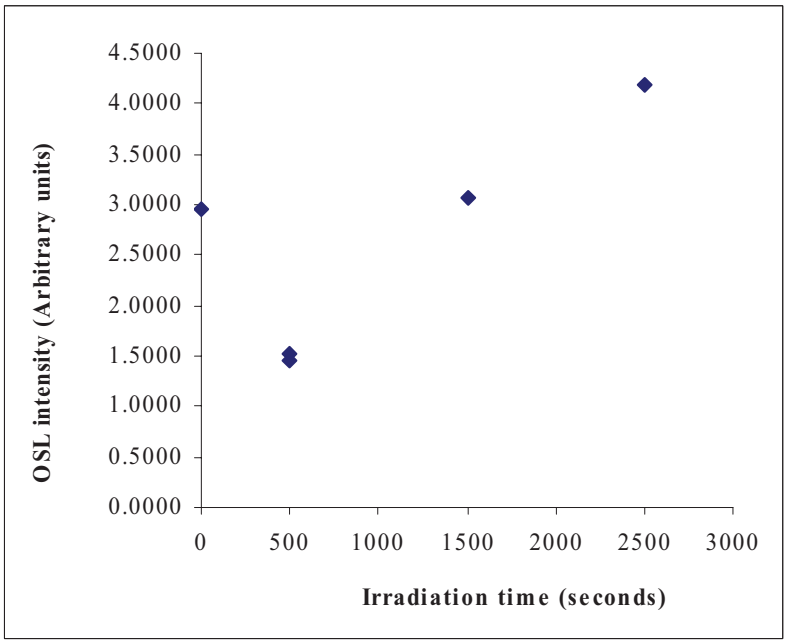

Figure 3.2 Example of a SAR growth curve obtained for aliquot 2 of sample X2566. In this instance, the interpolated palaeodose was equivalent to 1526.41±132.09 sec (72.81±6.30 Gy). The excellent recycling value (1.04) obtained for a repeat measurement of the first dose step provides further confidence in the SAR measurement procedure.

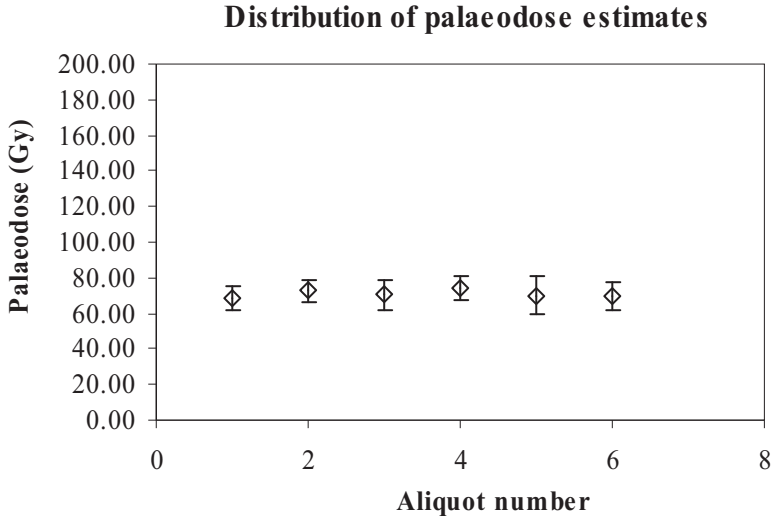

Figure 3.3 Distribution of palaeodose estimates obtained for six aliquots prepared from coarse grains of quartz extracted from sample X2566 and resulting in a weighted mean estimate of 71.05 ± 1.69 Gy. For most samples, the observed inter-aliquot variation was low and the good reproducibility between replicate measurements provides additional confidence in the palaeodose estimates.

4 References

Adamiec G. and Aitken M. J. 1998 Dose-rate conversion factors: update. *Ancient TL*, 16, 37-50.

Aitken M. J. 1985 Thermoluminescence Dating. Academic Press, London.

Aitken M. J. 1998 *Introduction to optical dating*. Oxford University Press, Oxford.

Banerjee D., Murray A. S., Bøtter-Jensen L. and Lang A. 2001 Equivalent dose estimation using a single aliquot of polymineral fine grains. *Radiation Measurements*, 33, 73-94.

Huntley D. J., Godfrey-Smith D. I and Thewalt M. L. W. 1985 Optical dating of sediments. *Nature* 313, 105-107.

Mejdahl V. 1979 Thermoluminescence dating: beta dose attenuation in quartz grains. *Archaeometry*, 21, 61-73.

Murray A. S. and Wintle A. G. 2000 Luminescence dating of quartz using an improved single-aliquot regenerative-dose protocol. *Radiation Measurements* 32, 57-73.

Owen L. A., Mitchell W. A., Bailey R. M., Coxon P. and Rhodes E. J. 1997 Style and timing of glaciation in the Lahul Himalaya, northern India: a frame work for reconstructing Late Quaternary palaeoclimatic change in the western Himalayas. *Journal of Quaternary Science*, 12, 83-109.

Prescott J. R. and Hutton J. T. 1994 Cosmic ray contributions to dose rates for luminescence and ESR dating: large depths and long term time variations. *Radiation Measurements* 23, 497-500.

Rhodes E. J. 1988 Methodological considerations in the optical dating of quartz. *Quaternary Science Reviews* 7, 395-400.

Rhodes E. J., Bronk-Ramsey C., Outram Z., Batt C., Willis L., Dockrill S. Batt C. and Bond J. 2003 Bayesian methods applied to the interpretation of multiple OSL dates: high precision sediment age estimates from Old Scatness Broch excavations, Shetland Isles. *Quaternary Science Reviews*, 22, 1231-1244.

Smith B. W., Aitken M. J., Rhodes, E. J., Robinson P. D. and Geldard, D. M. 1986 Optical dating: methodological aspects. *Radiation Protection Dosimetry* 17, 229-233.

Smith B. W., Rhodes E. J., Stokes S., Spooner N. A. and Aitken M. J. 1990 Optical dating of sediments: initial results from Oxford. *Archaeometry*, 32, 19-31.

Stokes S., Thomas D. S. G. and Washington R. W. 1997 Multiple episodes of aridity in southern Africa since the last interglacial period. *Nature* 388, 154-159.

Zimmermann, D.W. 1971 Thermoluminescent dating using fine grains from pottery. Archaeometry, 13, 29-52.

Appendix 1: Details of radioactivity data and age calculations

Sample name	BLNG05-01	BLNG05-03	BLNG05-05	BURN05-01	BURN05-03
Laboratory code	**X2447**	**X2449**	**X2451**	**X2455**	**X2457**
Palaeodose (Gy)	143.06	197.61	127.16	220.31	126.56
Total uncertainty	4.693	18.497	5.397	22.153	10.849
Measured error	3.72	18.07	4.76	21.71	10.55
Grain size					
Min. grain size (μm)	180	180	180	125	180
Max grain size (μm)	255	255	255	180	255
Measured concentrations					
standard fractional error	0.050	0.050	0.050	0.050	0.050
% K	0.598	1.179	0.847	1.428	0.407
error (%K)	0.030	0.059	0.042	0.071	0.020
Th (ppm)	2.000	3.400	1.300	4.600	2.300
error (ppm)	0.100	0.170	0.065	0.230	0.115
U (ppm)	0.600	0.800	0.400	1.100	0.400
error (ppm)	0.030	0.040	0.020	0.055	0.020
Cosmic dose calculations					
Depth (m)	1.730	2.270	4.650	1.600	1.000
error (m)	0.100	0.100	0.100	0.100	0.100
Average overburden density (g.cm^3)	1.900	1.900	1.900	1.900	1.900
error (g.cm^3)	0.100	0.100	0.100	0.100	0.100
Latitude (deg.), north positive	51	51	51	50	50
Longditude (deg.), east positive	1	1	1	1	1
Altitude (m above sea-level))	-8	-8	-8	3	2
Geomagnetic latitude	53.6	53.6	53.6	52.6	52.6
Dc (Gy/ka), 55N G.lat, 0 km Alt.	0.167	0.156	0.117	0.170	0.184
error	0.016	0.013	0.009	0.016	0.023
Cosmic dose rate (Gy/ka)	0.167	0.156	0.117	0.170	0.184
error	0.015	0.013	0.009	0.016	0.023
Moisture content					
Moisture (water / wet sediment)	0.050	0.130	0.060	0.170	0.080
error	0.030	0.050	0.030	0.050	0.030
Total dose rate, Gy/ka	**0.97**	**1.48**	**1.05**	**1.77**	**0.77**
error	**0.05**	**0.11**	**0.07**	**0.13**	**0.04**
% error	**5.49**	**7.28**	**6.35**	**7.24**	**5.49**
AGE (ka)	**147.07**	**133.66**	**121.52**	**124.79**	**164.61**
error	**9.40**	**15.85**	**9.29**	**15.46**	**16.76**

Sample name	**CG05-01**	**CG05-02**	**CG05-03**	**CG05-05**	**DOGF05-02**
Laboratory code	**X2459**	**X2460**	**X2461**	**X2463**	**X2466**
Palaeodose (Gy)	148.67	132.50	176.59	145.39	106.92
Total uncertainty	5.154	19.006	14.895	12.12	15.43
Measured error	4.21	18.82	14.47	11.77	15.28
Grain size					
Min. grain size (μm)	180	180	180	180	255
Max grain size (μm)	255	255	255	255	355
Measured concentrations					
standard fractional error	0.050	0.050	0.050	0.050	0.050
% K	0.332	0.220	0.270	0.310	0.160
error (%K)	0.017	0.011	0.014	0.016	0.008
Th (ppm)	1.800	1.900	3.700	2.900	1.100
error (ppm)	0.090	0.095	0.185	0.145	0.055
U (ppm)	0.300	0.400	1.000	0.600	0.300
error (ppm)	0.015	0.020	0.050	0.030	0.015
Cosmic dose calculations					
Depth (m)	3.950	3.950	3.200	3.900	1.700
error (m)	0.100	*0.500*	*0.500*	0.250	0.250
Average overburden density (g.cm^3)	1.900	1.900	1.900	1.900	1.900
error (g.cm^3)	0.100	0.100	0.100	0.100	0.100
Latitude (deg.), north positive	52	52	52	52	52
Longditude (deg.), east positive	1	1	1	1	1
Altitude (m above sea-level))	8	8	8	8	12
Geomagnetic latitude	54.5	54.5	54.5	54.5	54.5
Dc (Gy/ka), 55N G.lat, 0 km Alt.	0.127	0.127	0.139	0.128	0.168
error	0.010	0.019	0.024	0.012	0.028
Cosmic dose rate (Gy/ka)	0.127	0.127	0.139	0.128	0.168
error	0.010	0.019	0.024	0.012	0.028
Moisture content					
Moisture (water / wet sediment)	0.050	0.050	0.050	0.070	0.120
error	0.030	0.030	0.030	0.030	0.050
Total dose rate, Gy/ka	**0.61**	**0.54**	**0.85**	**0.72**	**0.42**
error	**0.03**	**0.03**	**0.04**	**0.04**	**0.03**
AGE (ka)	**242.82**	**245.64**	**208.36**	**202.96**	**253.66**
error	**15.10**	**37.80**	**20.73**	**19.64**	**41.82**

Sample name	**DOGF05-03**	**MLF05-01**	**CLBG05-01**	**CLBG05-03**	**CLBG05-05**
Laboratory code	**X2467**	**X2478**	**X2553**	**X2555**	**X2557**
Palaeodose (Gy)	221.68	240.39	188.40	205.26	191.48
Total uncertainty	14.32	13.917	9.252	12.939	12.406
Measured error	13.62	13.06	8.45	12.27	11.80
Grain size					
Min. grain size (μm)	180	180	180	180	180
Max grain size (μm)	255	255	255	255	255
Measured concentrations					
standard fractional error	0.050	0.050	0.050	0.050	0.050
% K	0.400	0.420	0.560	0.910	0.840
error (%K)	0.020	0.021	0.028	0.046	0.042
Th (ppm)	2.900	5.300	2.300	5.100	3.800
error (ppm)	0.145	0.265	0.115	0.255	0.190
U (ppm)	0.600	2.200	0.800	1.200	1.100
error (ppm)	0.030	0.110	0.040	0.060	0.055
Cosmic dose calculations					
Depth (m)	0.950	4.200	1.300	1.050	1.700
error (m)	0.100	0.100	0.100	0.100	0.100
Average overburden density (g.cm^3)	1.900	1.900	1.900	1.900	1.900
error (g.cm^3)	0.100	0.100	0.100	0.100	0.100
Latitude (deg.), north positive	52	51	51	51	51
Longditude (deg.), east positive	1	0	0	1	1
Altitude (m above sea-level))	12	16	10	10	10
Geomagnetic latitude	54.5	53.8	53.8	53.6	53.6
Dc (Gy/ka), 55N G.lat, 0 km Alt.	0.185	0.123	0.177	0.183	0.168
error	0.024	0.009	0.019	0.022	0.016
Cosmic dose rate (Gy/ka)	0.185	0.124	0.177	0.183	0.168
error	0.024	0.009	0.019	0.022	0.016
Moisture content					
Moisture (water / wet sediment)	0.090	0.060	0.100	0.150	0.130
error	0.030	0.030	0.030	0.050	0.050
Total dose rate, Gy/ka	**0.84**	**1.32**	**0.96**	**1.43**	**1.30**
error	**0.04**	**0.06**	**0.05**	**0.10**	**0.09**
% error	**5.30**	**4.82**	**5.28**	**6.71**	**6.73**
AGE (ka)	**265.00**	**181.55**	**196.10**	**143.33**	**147.52**
error	**22.15**	**13.68**	**14.14**	**13.20**	**13.78**

Sample name	**CXTN05-01**	**CXTN05-03**	**CXTN05-05**	**KMP05-02**	**NHFM05-01**
Laboratory code	**X2559**	**X2561**	**X2563**	**X2566**	**X2580**
Palaeodose (Gy)	2.11	200.90	169.38	71.05	81.22
Total uncertainty	0.313	7.346	11.778	1.687	3.412
Measured error	0.31	6.15	11.28	0.91	3.00
Grain size					
Min. grain size (μm)	180	180	180	180	180
Max grain size (μm)	255	255	255	255	255
Measured concentrations					
standard fractional error	0.050	0.050	0.050	0.050	0.050
% K	0.370	0.290	0.400	0.523	0.639
error (%K)	0.019	0.015	0.020	0.026	0.032
Th (ppm)	4.600	3.700	2.900	2.600	4.300
error (ppm)	0.230	0.185	0.145	0.130	0.215
U (ppm)	1.300	1.000	0.600	0.700	0.900
error (ppm)	0.065	0.050	0.030	0.035	0.045
Cosmic dose calculations					
Depth (m)	0.560	1.900	1.150	1.160	0.840
error (m)	0.100	0.100	0.100	0.100	0.100
Average overburden density (g.cm^3)	1.900	1.900	1.900	1.900	1.900
error (g.cm^3)	0.100	0.100	0.100	0.100	0.100
Latitude (deg.), north positive	51	51	51	51	51
Longditude (deg.), east positive	0	0	0	1	1
Altitude (m above sea-level))	19	18	18	5	23
Geomagnetic latitude	53.8	53.8	53.8	53.6	53.6
Dc (Gy/ka), 55N G.lat, 0 km Alt.	0.195	0.164	0.180	0.180	0.188
error	0.038	0.015	0.020	0.020	0.026
Cosmic dose rate (Gy/ka)	0.196	0.164	0.181	0.180	0.189
error	0.038	0.015	0.020	0.020	0.026
Moisture content					
Moisture (water / wet sediment)	0.050	0.080	0.060	0.110	0.150
error	0.030	0.030	0.030	0.030	0.050
Total dose rate, Gy/ka	**1.12**	**0.86**	**0.86**	**0.92**	**1.12**
error	**0.06**	**0.04**	**0.04**	**0.05**	**0.07**
% error	**5.53**	**4.64**	**5.14**	**5.27**	**6.59**
AGE (ka)	**1.88**	**232.64**	**197.54**	**77.23**	**72.63**
error	**0.30**	**13.75**	**17.09**	**4.47**	**5.68**

Sample name	**RHLLF05-01**	**WTHF05-02**	**DGFM05-03**	**MCKY05-01**	**NHL05-01**
Laboratory code	**X2582**	**X2588**	**X2589**	**X2591**	**X2672**
Palaeodose (Gy)	227.07	296.60	292.55	268.93	171.79
Total uncertainty	10.404	9.594	18.765	12.533	14.318
Measured error	9.36	7.54	17.83	11.32	13.90
Grain size					
Min. grain size (μm)	180	180	180	180	180
Max grain size (μm)	255	255	255	255	255
Measured concentrations					
standard fractional error	0.050	0.050	0.050	0.050	0.050
% K	0.623	1.303	0.764	0.913	*0.090*
error (%K)	0.031	0.065	0.038	0.046	0.005
Th (ppm)	7.600	7.600	6.400	9.400	2.400
error (ppm)	0.380	0.380	0.320	0.470	0.120
U (ppm)	2.100	1.800	1.900	2.400	0.700
error (ppm)	0.105	0.090	0.095	0.120	0.035
Cosmic dose calculations					
Depth (m)	1.900	1.170	2.450	2.400	1.250
error (m)	0.100	0.100	0.100	0.100	0.100
Average overburden density (g.cm^3)	1.900	1.900	1.900	1.900	1.900
error (g.cm^3)	0.100	0.100	0.100	0.100	0.100
Latitude (deg.), north positive	51	51	51	51	51
Longditude (deg.), east positive	0	0	1	1	0
Altitude (m above sea-level))	30	42	32	12	21
Geomagnetic latitude	53.8	53.8	53.6	53.6	53.8
Dc (Gy/ka), 55N G.lat, 0 km Alt.	0.164	0.180	0.153	0.154	0.178
error	0.015	0.020	0.013	0.013	0.019
Cosmic dose rate (Gy/ka)	0.165	0.181	0.153	0.154	0.179
error	0.015	0.020	0.013	0.013	0.019
Moisture content					
Moisture (water / wet sediment)	0.070	0.180	0.100	0.150	*0.050*
error	0.030	0.050	0.030	0.050	0.030
Total dose rate, Gy/ka	**1.65**	**1.93**	**1.59**	**1.89**	**0.57**
error	**0.08**	**0.13**	**0.08**	**0.12**	**0.03**
% error	**4.85**	**6.81**	**4.99**	**6.55**	**5.03**
AGE (ka)	**137.34**	**153.82**	**183.92**	**142.59**	**300.16**
error	**9.17**	**11.60**	**14.94**	**11.46**	**29.23**

Sample name	**RHLLF05-05**	**SLM05-02**
Laboratory code	**X2674**	**X2677**
Palaeodose (Gy)	242.03	295.91
Total uncertainty	23.122	16.722
Measured error	22.61	15.64
Grain size		
Min. grain size (μm)	180	180
Max grain size (μm)	255	255
Measured concentrations		
standard fractional error	0.050	0.050
% K	0.220	0.500
error (%K)	0.011	0.025
Th (ppm)	3.700	7.100
error (ppm)	0.185	0.355
U (ppm)	1.200	1.700
error (ppm)	0.060	0.085
Cosmic dose calculations		
Depth (m)	0.650	1.600
error (m)	0.100	0.100
Average overburden density (g.cm^3)	1.900	1.900
error (g.cm^3)	0.100	0.100
Latitude (deg.), north positive	51	51
Longditude (deg.), east positive	0	1
Altitude (m above sea-level))	25	43
Geomagnetic latitude	53.8	53.6
Dc (Gy/ka), 55N G.lat, 0 km Alt.	0.193	0.170
error	0.033	0.016
Cosmic dose rate (Gy/ka)	0.193	0.171
error	0.033	0.016
Moisture content		
Moisture (water / wet sediment)	*0.050*	0.070
error	0.030	0.030
Total dose rate, Gy/ka	**0.90**	**1.43**
error	**0.05**	**0.07**
% error	**5.52**	**4.80**
AGE (ka)	**268.64**	**206.45**
error	**29.64**	**15.30**

Appendix 2: Dose rate determination

Radiation dose is measured in energy units of Gray (Gy), the standard SI unit of absorbed dose (1 Gy = 1 Joule/kg). The measurement of dose rate (or annual dose) can be made using a variety of different methods. For most samples, the majority of the environmental dose rate is due to the radioactive decay of unstable isotopes of potassium (K), uranium (U) and daughter isotopes, and thorium (Th) and daughter isotopes. A further small fraction comes from the cosmic dose rate, and is a function of altitude, geomagnetic latitude, and overburden thickness and density (Prescott and Hutton 1994). Water content attenuates the environmental dose rate, and uncertainties in the average of this value over the burial period may often form a significant contribution to the overall uncertainty in the age estimate.

In-situ gamma spectrometry

Portable gamma spectrometer readings may be taken at each sampling location. The probe (housing an NaI scintillator crystal) is inserted into a deepened hole excavated following the retrieval of the OSL sample. Measurements typically take up to one hour and result in the direct estimation of the total *in situ* gamma radiation field. The spectra are also used to estimate contributions from U, Th, and K individually. Through comparison to known concentration standards, quantitative estimates of U, Th, and K concentrations are made.

Neutron Activation Analysis

A representative sub-sample (typically 10-20g, though as little as 80mg may be used with specialised procedures) of the sample is sent for commercial analysis. The analysis involves an initial (neutron) irradiation of each sample. This causes the creation of many new short-lived isotopes whose concentration depend on the bulk chemical composition of the original sample. This leaves the samples in a highly unstable (ie radioactive) state. The different gamma emissions from the radioactive decay of the sample are then measured using high resolution gamma-spectrometry. These measurements yield estimates of U, Th, and K concentration. The measurement of K and Th are usually precise, though samples with low levels of U may be below the detection limit for this element, depending on the interferences from other isotopes. The direct measurement of a small volume renders this method very well suited for the estimation of beta dose rate.

Moisture content of the sample

Moisture within the pore spaces of sediments absorbs α, β and γ-radiation. As a result, less is absorbed by the mineral grains. It is therefore important to assess the present day water content of the sediment and to make some assessment of the variability of moisture throughout the burial period of the sample. The moisture correction factors outlined in Aitken (1985) and taken from Zimmermann (1971) are used in the age calculation (Appendix 1).

Cosmic dose rate

The contribution of cosmic radiation to the total dose rate is calculated as a function of (geomagnetic) latitude, altitude, burial depth, and average over-burden density, according to the formulae of Prescott and Hutton (1994).

Radiation attenuation factors

For coarse grains, the portion of the sample that receives an α-dose is removed by HF etching. Therefore, no consideration of the α-dose is made during the age calculation. β-particles (electrons) are significantly attenuated (ie a large fraction of the energy is absorbed) as the β-particle passes through a grain. Account of this effect is needed in order to correctly estimate the dose received by the 'average' grain. The so-called 'attenuation factors' are taken from the empirical work of Mejdahl (1979).

The γ-dose is assumed to be unaffected by attenuation as the penetration of gamma-rays through sediments is several orders of magnitude greater than ($\sim 10^5$ times) the size of individual grains. Consequently, no attenuation factors are applied to the γ-dose.

Results for the U, Th (ppm), and K (%) concentration of each sample, together with the other parameters used in the age calculation, are provided in Appendix 1.

Appendix 3: Statistics and error calculation

The calculated age depends on the estimate of total absorbed dose (D_e) and the dose rate (D_R). Both of these estimates have uncertainties associated with them. This appendix gives general details of how the 'error' (the statistical uncertainty) is calculated for each term and combined with the errors on other terms to give an overall estimate of uncertainty on the OSL age estimate.

Palaeodose estimation

As described in a previous section (Figure 2.1), individual estimates of palaeodose also referred to as D_e are obtained from each of the aliquots (sub-samples) measured, using the SAR technique. The value of the D_e is obtained by interpolating between the points of the dose response curve. Statistical uncertainties are calculated for each of the individual points and also on the interpolated value of D_e. Typically, 12 aliquots are measured for each sample.

Each of the points on the growth curve is defined as:

$$I(\beta)_i = \frac{L_i - f \cdot l_i}{S_i - f \cdot s_i \cdot} \qquad \text{Eq.1}$$

where L_i is the integrated (initial) OSL from the regeneration dose and l_i is the measured background signal, S_i is the integrated (initial) OSL from the test dose (see Section 3) and s_i is the background; f is a scaling factor included to take account of the difference in duration of the L_i,S_i and l_i,s_i measurements.

The error on each dose-response data point (see Figure 2.1) is calculated by propagating 'counting statistics' errors (assuming Poisson statistics) from the integration of raw OSL data. The error on each term in Equation 1 is given by the square-root of the value. For example, the range for L_i is given by $L_i \pm \sqrt{L_i}$. The errors on each value are propagated in the standard way (see below) to give the uncertainty of $I(\beta)_i$.

In cases where the dose response can be (locally) approximated by a straight line, a weighted least squares linear fit is used. The errors in this case are calculated analytically using standard formulae.

In cases where the dose response is significantly non-linear, a single saturating exponential function is used to describe the dose response (a Simplex algorithm is used for fitting in this case). Occasionally an extra linear term is added to the exponential term in order to better describe the form of the dose response, although this is not commonly necessary. The uncertainty for non-linear fitting is calculated using a Monte-Carlo method in which 'random samples' of the dose response data are taken (assuming normally distributed probabilities) and used to obtain the palaeodose value. The spread in these values is then used to calculate

the error on the mean palaeodose for each aliquot, giving a range for each palaeodose of $D_{ei} \pm \sigma D_{ei}$

Once the individual D_e values have been obtained from each aliquot (and the associated uncertainties calculated) the values are grouped to give a final overall estimate of D_e. The final D_e estimate is calculated using a weighted average. The weight of each D_e is referred to as w_i and defined as:

$$w_i = \frac{1}{\sigma D_{ei}^2} \Bigg/ \sum_i \frac{1}{\sigma D_{ei}^2} \qquad \text{Eq.2}$$

The weighted mean is defined as:

$$\overline{D}_e = \sum_i D_{ei} \cdot w_i \qquad \text{Eq.3}$$

The weighted standard error, $\hat{\sigma}_{\bar{x}w}$, is calculated from:

$$\hat{\sigma}_{\bar{x}w} = \sqrt{\frac{\sum_i w_i \left(D_{ei} - \overline{D}_e\right)}{1 - \frac{1}{n}}} \Bigg/ \sqrt{n} \qquad \text{Eq.4}$$

where n is the number of aliquots. The range of the weighted mean D_e is then defined as:

$$\overline{D}_e \pm \hat{\sigma}_{\bar{x}w} \qquad \text{Eq.5}$$

Slight modifications to the approach outlined above are made in special circumstances, though in most cases this description is sufficient.

Dose rate

The errors on the dose rate are due to errors in a range of values, for example, the concentration of U, Th and K, as well as the water content of the sample. The individual components of the dose rate calculation are shown in Appendix 1. The uncertainty on the overall dose rate is calculated by combing the uncertainties according to the standard propagation formula given below.

Age calculation

The calculated age is obtained from dividing the mean D_e (Eq.3) by the total dose rate (Appendix 1). The uncertainty on the final age estimate is calculated using the error propagation formula given below. All calculations were performed using software developed within the laboratory.

Standard error propagation

If a calculated value (y) is calculated using a function (f) which contains terms x_1, x_2, x_3.... x_n, then,

$$y = f(x_1, x_2, x_3 ... x_n) \qquad \text{Eq.6}$$

Each term (x_i) has an associated uncertainty with a range expressed as $x_i \pm \sigma_{xi}$. The overall error of y can be calculated through the addition of the partial derivatives of y with respect to each term. Formally, this is written as:

$$\sigma_y = \sqrt{\sum_i \left(\frac{\partial y}{\partial x_i} \cdot \sigma_{xi} \right)^2} \qquad \text{Eq.7}$$

giving a range for y as $y \pm \sigma_{Y.}$